Regenerative Therapy 24 (2023) 256–266

Contents lists available at ScienceDirect

Regenerative Therapy

journal homepage: http://www.elsevier.com/locate/reth

Original Article

Transcriptomic analysis of hepatocytes reveals the association between ubiquitin-specific peptidase 1 and yes-associated protein 1 during liver regeneration

Yalei Zhao [a, b, 1], Fen Zhang [b, 1], Xiaoli Zhang [a, 1], Zuhong Li [b], Qian Li [b], Tianzhi Ni [a], Ruojing Wang [a], Liangru Liu [a], Yingli He [a, **], Yingren Zhao [a, *]

[a] Department of Infectious Diseases, The First Affiliated Hospital of Xi'an Jiaotong University, Xi'an, China
[b] State Key Laboratory for Diagnosis and Treatment of Infectious Diseases, National Clinical Research Center for Infectious Diseases, Collaborative Innovation Center for Diagnosis and Treatment of Infectious Diseases, The First Affiliated Hospital, College of Medicine, Zhejiang University, Hangzhou, China

ARTICLE INFO

Article history:
Received 15 April 2023
Received in revised form
12 June 2023
Accepted 10 July 2023

Keywords:
Ubiquitin specific peptidase 1
Yes-associated protein 1
Liver regeneration
Hepatocyte proliferation
Partial hepatectomy

ABSTRACT

Objectives: The liver has an excellent ability to regenerate, and disrupted liver regeneration after various injuries leads to an unfavorable prognosis for patients. In this study, we sought to identify novel therapeutic hallmarks that are associated with yes-associated protein 1 (YAP1)-mediated hepatocyte proliferation during the process of liver regeneration.

Methods: Partial hepatectomy was conducted to induce liver regeneration in rats. Primary hepatocytes were isolated and cultured. Hepatocyte proliferation was assessed using immunohistochemistry staining, and expression of YAP1 was detected. RNA sequencing and bioinformatics analysis were used to search for potential regulators of YAP1. The association between ubiquitin-specific peptidase 1 (USP1) and YAP1 was validated using *in vivo* and *in vitro* experiments.

Results: YAP1 was significantly elevated in regenerative hepatocytes, especially in the nucleus. Knockdown of YAP1 using small interfering RNA or pharmacological inhibition using verteporfin significantly attenuated the proliferation of hepatocytes. The bioinformatics analysis results revealed that USP1 was associated with YAP1-mediated hepatocyte proliferation during liver regeneration. ML-323, a specific inhibitor of USP1-USP1 associated factor 1 (UAF1), significantly decreased the expression of YAP1, Cyclin D1, and proliferating cell nuclear antigen, while these decreased expressions could be rescued by YAP1 overexpression. Furthermore, ML-323 treatment significantly inhibited liver regeneration following partial hepatectomy.

Conclusions: In conclusion, we identified USP1 as a novel biomarker that is associated with YAP1-mediated hepatocyte proliferation in liver regeneration. Pharmacological inhibition of USP1 by ML-323 substantially impairs hepatocyte proliferation during liver regeneration.

1. Introduction

In recent years, regenerative medicine has greatly progressed with the development of biomedicine [1]. Meanwhile, accumulating evidence has reported the molecular basis and potential approaches of organ regeneration [2,3]. The successful activation of regenerative responses is crucial to maintaining organ function after various insults, while failure of regeneration leads to organ malfunction [4]. Thus, of notable interest is a means to therapeutically activate these regenerative responses and to effectively monitor the process of regeneration [5].

Healthy livers have a remarkable regenerative capacity to ensure liver tissue maintenance via the "hepatostat," allowing them to recover from injuries [6]. However, this regenerative capacity declines in aging and chronically diseased livers, so they cannot regenerate efficiently [6–9]. Liver regeneration is a highly complex process involving multiple signal pathways, such as the WNT pathway and the Hippo pathway [4,10,11]. Interestingly, the hepatic

* Corresponding author.
** Corresponding author.
E-mail addresses: heyingli2000@xjtu.edu.cn (Y. He), zhaoyingren@xjtu.edu.cn (Y. Zhao).
Peer review under responsibility of the Japanese Society for Regenerative Medicine.
[1] These authors contribute equally to this paper.

https://doi.org/10.1016/j.reth.2023.07.004

regeneration processes differ depending on the cause of injury [7]. There are mainly two diverse regeneration ways in these processes: self-replication and cell identity conversion of hepatic epithelial cells [12,13]. Although outstanding efforts have been made, the precise mechanisms underlying the regeneration processes are still not fully understood. Nevertheless, the Hippo pathway has gained a lot of attention due to its major role in liver biology [14]. Yes-associated protein 1 (YAP1), the downstream effector of the Hippo pathway, is critically involved in and heralded as a master regulator of liver regeneration, no matter hepatocyte replication or cell identity conversion [4]. A better understanding of the regulatory mechanisms of YAP1 may provide a keystone for the development of therapeutic strategies for liver regeneration. Thus, screening and identification of novel regulators of YAP1 have been areas of great interest. In this study, we focus on searching for novel therapeutic biomarkers that are associated with YAP1 during the process of liver regeneration. Our results confirmed the association between USP1 and YAP1 *in vitro* and *in vivo*.

2. Methods

2.1. Animals

Six-to eight-week-old male Sprague-Dawley rats were utilized in this study. Rats were housed under a 12-h light-dark cycle and fed ad libitum. The animal room was kept at a constant temperature (22 ± 2 °C) with 50% humidity. All of the animal experiments were approved by the Experimental Animal Ethics Committee of Xi'an Jiaotong University.

2.2. Materials

Verteporfin, a YAP1 inhibitor, was acquired from Selleck (Selleck, USA). ML-323, a USP1 inhibitor, was purchased from ABIxBIO (APExBIO, USA). BRL3A cells have been purchased at Procell (Procell Life Science&Technology Co.,Ltd., China). Antibodies used in this study include *anti*-USP1, *anti*-Ki67, anti-proliferating cell nuclear antigen (PCNA), anti-YAP1, *anti*-Cyclin D1, anti-ALB, anti-beta tubulin, and *anti*-GAPDH (Details shown in Supplemental Table S1).

2.3. Partial hepatectomy (PHx)

The procedure for PHx was carried out according to the previous study established by Higgins and Anderson [15]. For PHx, the middle and left liver lobes were removed after rats were anesthetized. In total, 28 rats were randomized to different treatment groups. Firstly, 16 rats were divided into the following groups: the pre-PHx group (treated without PHx) (n = 8) and the PHx-24 h group (24 h (h) after PHx) (n = 8). Of these, liver samples and blood samples were harvested from 5 rats in the pre-PHx group and 5 rats in the PHx-24 h group. Primary hepatocytes were isolated from 3 rats in the pre-PHx group and 3 rats in the PHx-24 h group. Then, 12 rats were divided into the following groups: the normal control group (NC) (n = 3), the Sham group (n = 3), the PHx group (n = 3), and the ML-323 group (n = 3). ML-323 was dissolved in phosphate buffer saline containing 5% dimethyl sulfoxide. For rats in the ML-323 group, 10 mg/kg of ML-323 was injected intraperitoneally 30 min after PHx. For rats in the PHx group, an equal volume of vehicle was delivered intraperitoneally at the same timepoints. All the regents were used immediately after dissolution in the animal experiments.

2.4. Primary hepatocyte isolation and cell culture

Primary hepatocytes were isolated according to our previous study [16]. Briefly, procedures were conducted as follows: The rats from the pre-PHx group and the PHx-24 h group were anesthetized. Ca^{2+}-free medium, which contained 1 μM ethylenediaminetetraacetic acid (Sigma-Aldrich, USA), was perfused through the portal vein *in situ*. After the blood was flushed, the perfusion medium was successively changed to the digestion medium I with 0.08% (w/v) dispase (Gibco, USA) and the digestion medium II with 0.05% (w/v) collagenase IV (Sigma-Aldrich, USA). Note that all the digestion mediums were kept at 37 °C during perfusion. While tiny cracks were observed on the liver surface, digestion was terminated. Then, the liver was resected and transferred to a cool buffer containing 0.1 g/L bovine serum albumin. Subsequently, the liver was gently minced, and the cells were purified by gradient centrifugation. Moreover, the primary hepatocytes were further purified with percoll (GE Healthcare, Sweden). For cell culture, Williams E medium (Sigma-Aldrich, USA) and collagen-I-coated plates were used. In addition, the Williams E medium was supplemented with 10% fetal bovine serum (FBS) (Gibco, USA), 1 × penicillin (100 units/mL)/streptomycin (100 μg/mL) (Sigma-Aldrich, USA), 0.1 mmol/L dexamethasone (Life Technologies, USA), 1 × insulin-transferrin-selenium (Life Technologies, USA), and 1 × L-glutamine (Life Technologies, USA).

2.5. Immunofluorescence staining

The primary hepatocytes from the pre-PHx group (pre-PHx-Hep) and the PHx-24 h group (PHx-24 h-Hep) were cultured on coverslips. Firstly, the cells were washed three times with phosphate buffer saline. Then, the cells were fixed in 4% paraformaldehyde at room temperature. After 15 min, the cells were washed and permeabilized with 0.5% Triton X-100. After 10 min, the cells were washed again and then blocked with 5% bovine serum albumin for 30 min. The cells were incubated with an antibody against albumin (details shown in Table S1) overnight at 4 °C. The next day, the cells were washed three times and then incubated with the secondary antibody at 37 °C for 1 h. Before examination, 4′,6-diamidino-2-phenylindole (DAPI) (Abcam, USA) was added and nuclei were stained.

2.6. Total, nuclear, and cytoplasmic protein extraction

To obtain total proteins of pre-PHx-Hep and PHx-24 h-Hep, RIPA lysis buffer (1 × protease inhibitor) (GenStar, China) (Beyotime Biotechnology, China). Total proteins were extracted and then quantified using BCA kits (Thermo Scientific, USA). To obtain proteins from the nuclear and cytoplasm, we used a commercial kit (Beyotime, China). Nuclear and cytoplasmic proteins of pre-PHx-Hep and PHx-24 h-Hep were extracted according to the manufacturer's protocol. Briefly, the cells were washed with phosphate buffer saline and centrifuged. Then, cytoplasmic protein extraction buffer A with 1 mM PMSF (Beyotime Biotechnology, China) was added to the centrifuged deposit. Fifteen minutes of lysis on ice. After that, cytoplasmic protein extraction buffer B was added, and lysis was on ice for 1 min. After vortexing and centrifugation (12000g, 4 °C) for 5 min, the supernatant was saved for further analysis (cytoplasmic protein). The centrifuged deposit was then treated with the nuclear protein extraction buffer. Thirty minutes of lysis on ice. After vortexing and centrifugation (12000g, 4 °C) for 10 min, the supernatant was saved for further analysis (nuclear protein).

2.7. siRNA transfection

SiRNA-YAP1 (5′-CUUAAAUCACAAUGAUCAG tt-3′ forward, and 5′-CUGAUCAUUGUGAUUUAAG tt-3′ reverse) and non-targeting control siRNA (NC-siRNA, 5′-UUCUCCGAACGUGUCACGUdTdT-3′ forward, and 5′-ACGUGACACGUUCGGAGAAdTdT-3′ reverse) were

obtained from Genomeditech Co. Ltd. (Genomeditech, Shanghai, China). To decrease YAP1 expression in PHx-24 h-Hep hepatocytes, 40 nmol/L siRNA-YAP1 or NC-siRNA was prepared and transfected into hepatocytes using INTERFERin (Polyplus transfection, New-York, USA) according to the manufacturer's protocol. After 48 h of transfection, the whole proteins of hepatocytes in different groups were extracted.

2.8. Western blot analysis

We used 4%–20% ExpressPlus™ PAGE Gels (GenScript, China) to separate approximately 20 μg proteins from different samples. Then, the proteins were transferred to polyvinylidene fluoride (PVDF) membranes. Subsequently, PVDF membranes were blocked for 15–30 min at room temperature using Quickblock™ buffer (Beyotime Biotechnology, China). After that, PVDF membranes were incubated with different primary antibodies (shown in Table S1). After incubation at 4 °C for overnight, PVDF membranes were rinsed with Tris-HCl buffer (containing 0.5% v/v T-ween) three times, and then incubated with different secondary antibodies (Abcam, USA) at room temperature. After 1 h, PVDF membranes were rinsed again and visualized with super ECL detection reagents (Yeasen, China).

2.9. Immunohistochemistry staining

Following deparaffinization of the liver paraffin sections, the liver sections were hydrated in various ethanol concentrations. Then, endogenous peroxidase was blocked with 3% hydrogen peroxide. After that, the liver sections were incubated with different primary antibodies at 4 °C overnight. The next day, the liver sections were rinsed with phosphate buffer saline and incubated with different secondary antibodies (Abcam, USA) at 37 °C for 1 h. After washing three times, we used a commercial kit which containing 3,3′-diaminobenzidine solution (Abcam, USA) for further incubation. Finally, the liver sections were photoed and saved for further analysis.

2.10. Cell culture of BRL3A cells

The rat liver BRL3A cells were purchased from Procell (Procell Life Science&Technology Co.,Ltd., China). The BRL3A cells were cultured in modified Eagle's medium (MEM) medium which contained 10% foetal bovine serum (GIBCO, USA), 100 U/mL penicillin and 100 μg/mL streptomycin (Gibco, USA). For inhibition of YAP1 activity *in vitro*, VP (1 μM) was used to treat cells for 24 h. We used ML-323 for the pharmacological intervention of USP1. According to our previous study, ML-323 was used at 50 μM [5]. For vehicle control (Ctrl), 0.1% DMSO was used. After culture for 24 h, the treatment was terminated.

2.11. RNA sequence and bioinformatics analysis

Total RNA was extracted using Trizol (Invitrogen, USA) and quantified using NanoDrop and an Agilent 2100 bioanalyzer (Thermo Fisher Scientific, USA). Equal amounts of RNA from different samples were used to construct a cDNA library. Oligo (dT)-attached magnetic beads were applied to enrich mRNA. Then, the mRNA was broken into short fragments. Subsequently, we used the short mRNA fragments as templates to synthesize the first-strand cDNA. Double-stranded cDNA was synthesized and then terminally repaired. Finally, poly A was added to the repaired fragments and ligated to adaptor sequences. Subsequently, we used the ligated products to construct cDNA libraries. After quality checks, the qualified cDNA libraries were sequenced by the MGI2000 platform (TSINGKE, China). After sequencing, raw data from different samples were obtained and then processed using Trimmomatic [17]. Based on gene expression, differentially expressed genes (DEGs) were identified (pre-PHx-Hep vs PHx-24 h-Hep: Fold change >2, P adj. <0.05). Several online analysis tools were used for further analysis. The volcano plot and heatmap were conducted using MetaboAnalyst (www.metaboanalyst.ca) and Bioinformatics (https://www.bioinformatics.com.cn/). The protein-protein interaction network analysis was conducted using STRING (http://string‐db.org) and Cytoscape software (Version 3.9.1). The Kyoto Encyclopedia of Genes and Genomes (KEGG) analysis and Gene Ontology (GO) analysis were conducted using the Database for Annotation, Visualization, and Integrated Discovery (DAVID 6.8, v6.8, https://david.ncifcrf.gov/home.jsp) and Bioinformatics (https://www.bioinformatics.com.cn/) [18].

2.12. Bioinformatics analysis of data from public databases

The LinkedOmics database (http://www.linkedomics.org/login.php) was utilized to search for differentially expressed genes positively correlated with YAP1 [19]. For Pearson correlation analysis, the TCGA-LIHC dataset (n = 371) was selected. In addition, correlation analysis between USP1 and YAP1 was further validated in the GEPIA database (http://gepia.cancer‐pku.cn) [20]. The Venn analysis was conducted using Venny 2.1.0 (https://bioinfogp.cnb.csic.es/tools/venny/index.html).

2.13. Infection of YAP1 overexpression lentivirus

To overexpress YAP1 in BRL3A cells, a lentivirus vector was constructed and obtained from Genomeditech Co. Ltd. (Genomeditech, China). The information for the lentivirus vector was shown in Fig. S1 and Table S2. The infection effects of YAP1-OE vectors with a multiplicity of infection (MOI) of 0–100 were evaluated. A MOI of 50 was chosen to infect BRL3A cells for 72 h. The cells in the negative control group were transfected with a control vector. YAP1 expression in BRL3A cells was analyzed using western blotting.

3. Statistical analysis

Data in the present study are shown as the mean ± SD. For the gene enrichment analysis in DAVID, Fisher's exact test was conducted. The differences between groups in *vitro* and *in vivo* experiments were detected using Student's *t tests*. $P < 0.05$ was statistically significant (*$P < 0.05$; **$P < 0.01$; ***, $P < 0.001$).

4. Results

4.1. Elevated expression of YAP1 during liver regeneration

In our previous study, we found that the hepatic expression levels of YAP1 were significantly elevated at 24 h and 48 h after PHx, which was paralleled with the proliferation of hepatocytes after PHx [5]. We evaluated the histological changes of the regenerating liver. H&E staining was performed, and no significant hepatocyte necrosis was observed. Expectedly, a significant increase in the number of YAP1-positive staining hepatocytes was observed in the regenerating liver (Fig. 1A). Moreover, the elevated hepatic expression of YAP1 in the PHx-24 h group was further confirmed by western blotting results (Fig. 1B–C). We next examined the proliferative markers of hepatocytes. At 24 h post-PHx, we observed an increased number of $PCNA^+$ hepatocytes and $Ki67^+$ hepatocytes. As previously reported, elevated YAP1 expression during liver regeneration stimulated hepatocytes to undergo epithelial-mesenchymal transition. Hepatocytes in regenerating livers may transiently lose or down-regulate their epithelial markers [21]. Thus, ELISA and immunofluorescence staining were performed to detect plasma

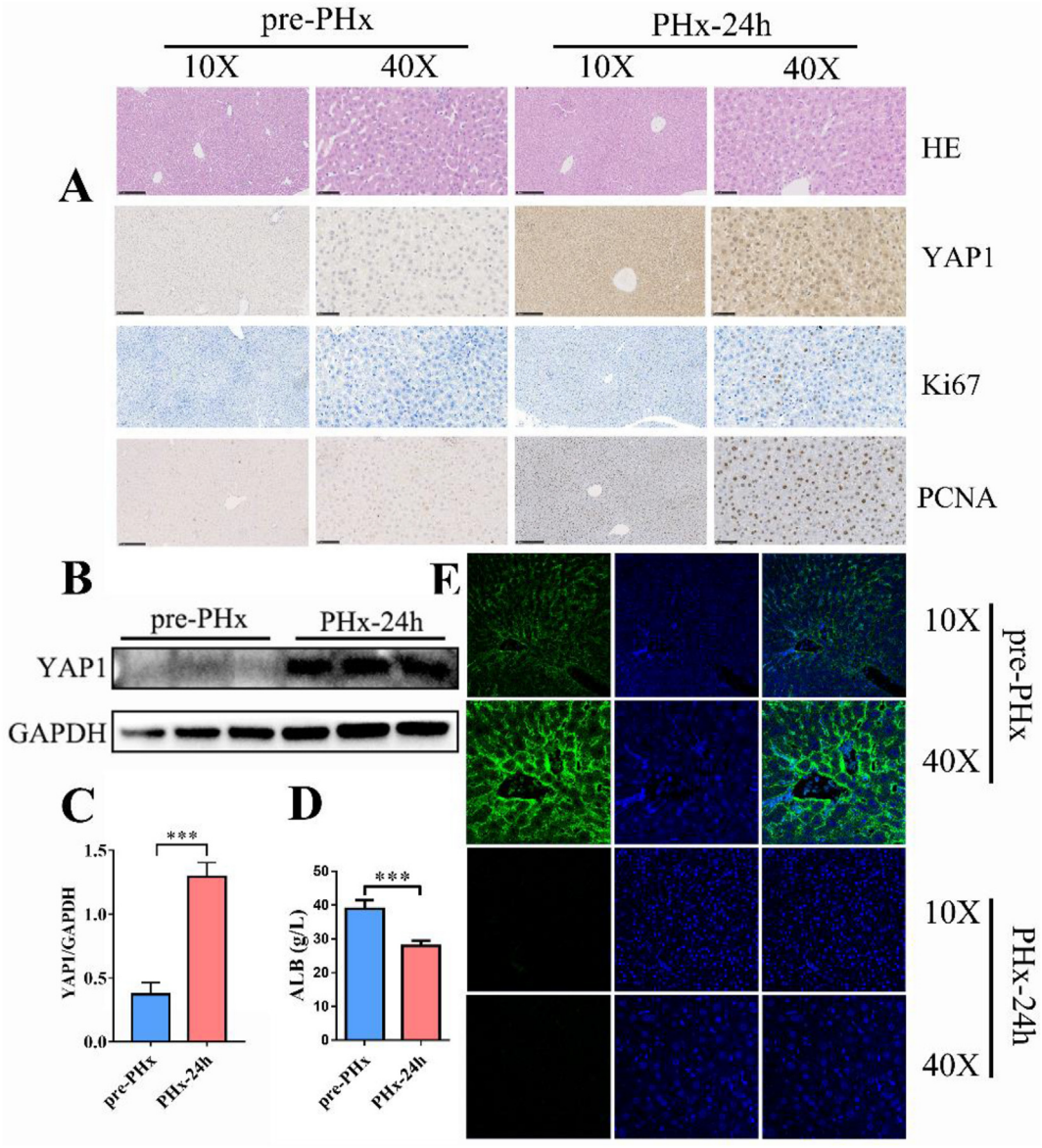

Fig. 1. Elevated hepatic expression of YAP1 during liver regeneration. (A). Histological changes, Ki67 staining, and PCNA staining in pre-PHx and PHx-24 h groups. 10X scale bar: 250 μm, 40X scale bar: 50 μm. (B–C). Protein expression levels of YAP1 in pre-PHx and PHx-24 h groups. ***P < 0.001. (D). Serum levels of ALB in pre-PHx and PHx-24 h groups. ***P < 0.001. (E). Immunocytofluorescense staining of hepatic ALB in pre-PHx and PHx-24 h groups. pre-PHx: before partial hepatectomy, PHx-24 h: 24 h post partial hepatectomy, HE: hematoxylin-eosin staining, PCNA: proliferating cell nuclear antigen, YAP1: yes-associated protein 1, ALB: albumin.

and hepatic albumin. Due to the loss of liver parenchyma and partial epithelial-mesenchymal transition of hepatocytes, a significant decrease in plasma and hepatic albumin was observed in the PHx-24 h group (Fig. 1D–E). In addition, we also obtained primary hepatocytes from both groups (pre-PHx-Hep and PHx-24 h-Hep) to further validate the expression of YAP1 during liver regeneration. As YAP1 activation was characterized by its nuclear localization, immunofluorescence was performed in primary hepatocytes to detect its expression and localization [22]. Consistently, we observed elevated YAP1 expression in the PHx-24 h-Hep cells, and it was mainly expressed in the nucleus (Fig. 2A). To further confirm these results, nuclear and cytoplasmic proteins were extracted, and western blotting was performed. Similarly, we found that the expression levels of YAP1 and PCNA were elevated in nuclear proteins (Fig. 2B). Taken together, these results demonstrated that YAP1 was activated and expressed in the nucleus 24 h post-PHx.

4.2. Knockdown or pharmacological inhibition of YAP1 impairs hepatocyte proliferation

Then, siRNA was transfected into PHx-24 h-Hep cells to knockdown the expression of YAP1. The transfection efficiency was evaluated, and 40 nM siRNA was used for further experiments (Fig. 2C). After transfection with si-YAP1, the expression levels of YAP1, Cyclin D1, and proliferating cell nuclear antigen (PCNA) in PHx-24 h-Hep were significantly decreased (Fig. 2D–E). Moreover, a specific YAP1 inhibitor (Verteporfin, VP) was used to treat BRL3A cells. Similarly, pharmacologically inhibiting YAP1 significantly decreased the expression levels of Cyclin D1 and PCNA in BRL3A cells (Fig. 2F–J). In addition, we assessed the extent of cell proliferation of BRL3A by using CCK8, and the results showed that VP treatment significantly impairs hepatocyte proliferation (Fig. 2K).

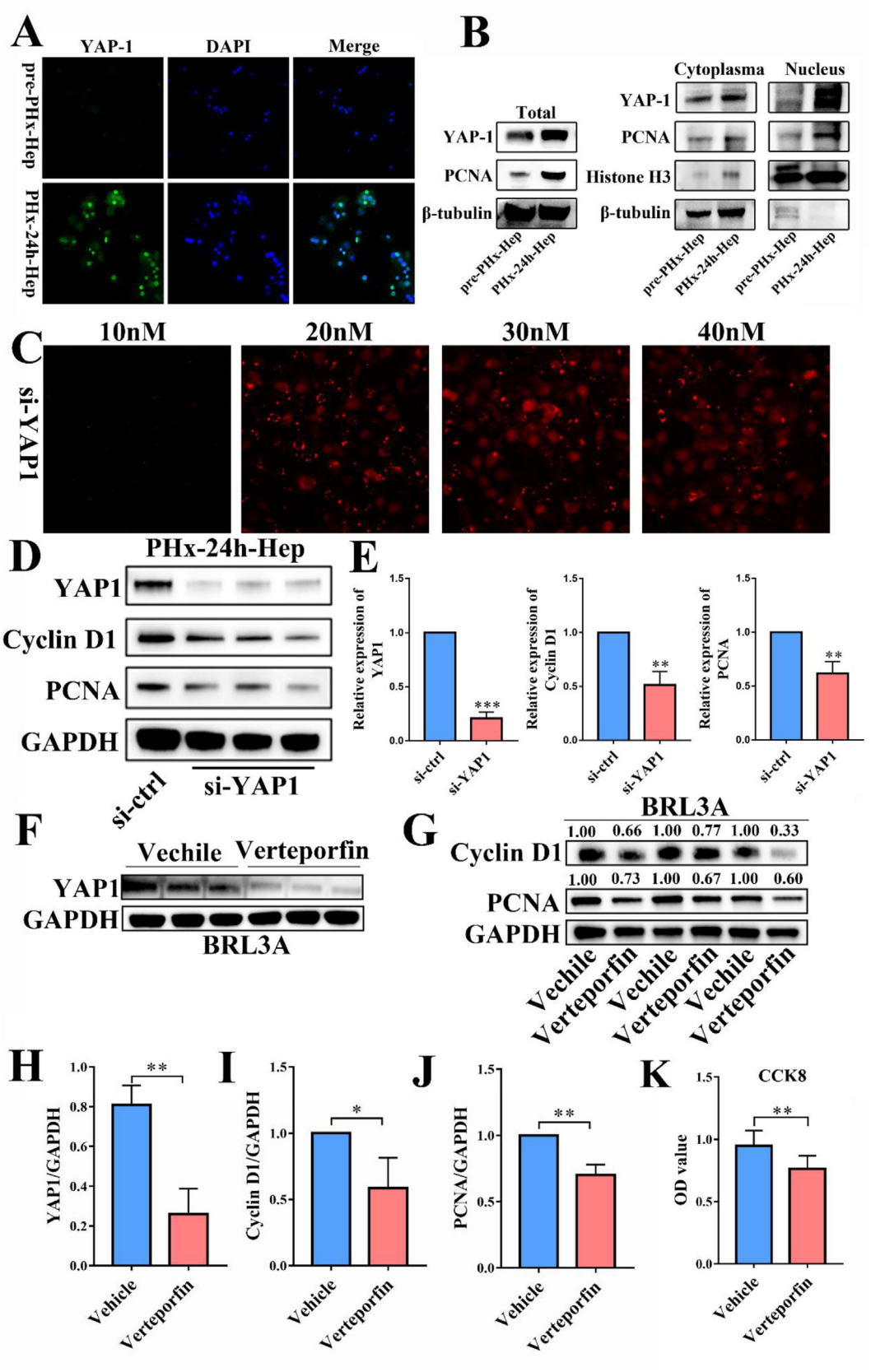

Fig. 2. Targeting YAP1 impairs hepatocyte proliferation. (A). Immunocytofluorescense staining of YAP1 in pre-PHx-Hep and PHx-24 h-Hep groups. Enlargement: 40X. (B). Whole, cytoplasma and nucleus expression of YAP1 and PCNA in pre-PHx-Hep and PHx-24 h-Hep groups. (C). siRNA transfection in PHx-24 h-Hep cells. Enlargement: 40X. (D–E). siRNA transfection decreased the expressions of YAP1, Cyclin D1 and PCNA in PHx-24 h-Hep cells. *P < 0.05, **P < 0.01, ***P < 0.001. (F–H). Expression of YAP1 in Vehicle and Verteporfin treated BRL3A cells. **P < 0.01. (G–J). Expression of Cyclin D1 and PCNA in Vehicle and Verteporfin treated BRL3A cells. *P < 0.05, **P < 0.01. (K). The cell proliferation of BRL3A in Vehicle and Verteporfin treated BRL3A cells. *P < 0.05.

4.3. Identification of the association between USP1 and YAP1 during liver regeneration

As the functional role of YAP1 has been well documented in previously published studies, we sought to search for novel therapeutic biomarkers of liver regeneration that are associated with YAP1. As noted above, YAP1 was low-expressed in the pre-PHx-Hep cells and highly expressed in the PHx-24 h-Hep cells. Thus, we first searched for the differentially up-expressed genes (DEG1) in the PHx-24 h-Hep cells based on the RNA-sequence results (PHx-24 h-Hep vs. pre-PHx-Hep, fold change >2, P adj. < 0.05) (Fig. 3A–B). Then, we used the LinkFinder module in the LinkedOmics database

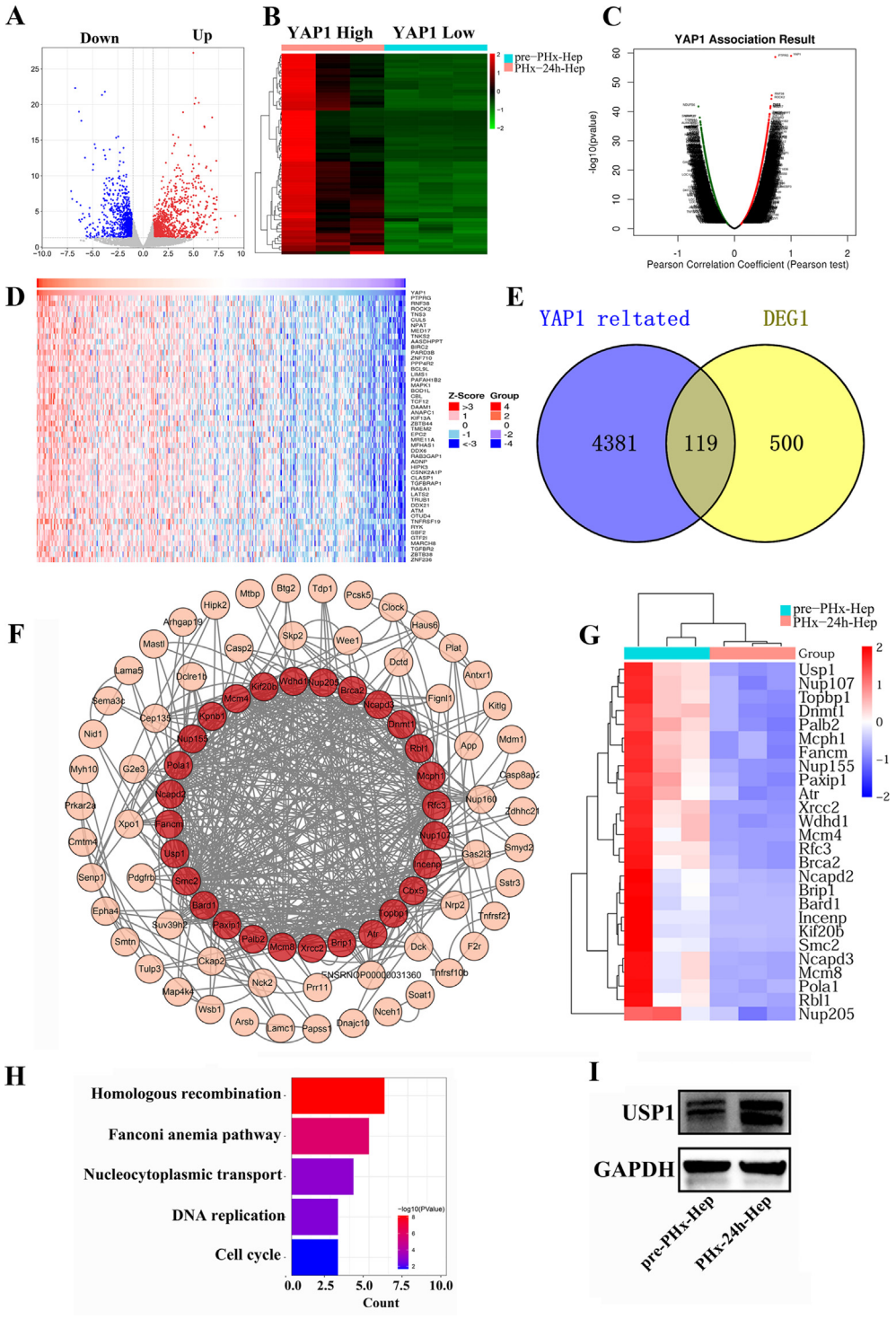

Fig. 3. Identification of the association between USP1 and YAP1 in hepatocyte proliferation. (A). Volcano Plot of differentially expressed genes between the pre-PHx-Hep group and the PHx-24 h-Hep group. (B). Heatmap of differentially expressed genes that were up-regulated in the PHx-24 h-Hep group. (C). Volcano Plot of differentially expressed genes that were correlated with YAP1 in the liver hepatocellular carcinoma (LIHC) dataset. (D). Heatmap of the top 50 differentially expressed genes that were positively correlated with YAP1 in the LIHC dataset. (E). Venn results showed the common genes between the YAP1 related genes and the DEG1. (F). PPI network of the identified 119 genes, hub genes were showed in red color. (G). Heatmap of the identified hub genes. (H). KEGG analysis of the identified hub genes. (I). Expression of USP1 in pre-PHx-Hep and PHx-24 h-Hep groups.

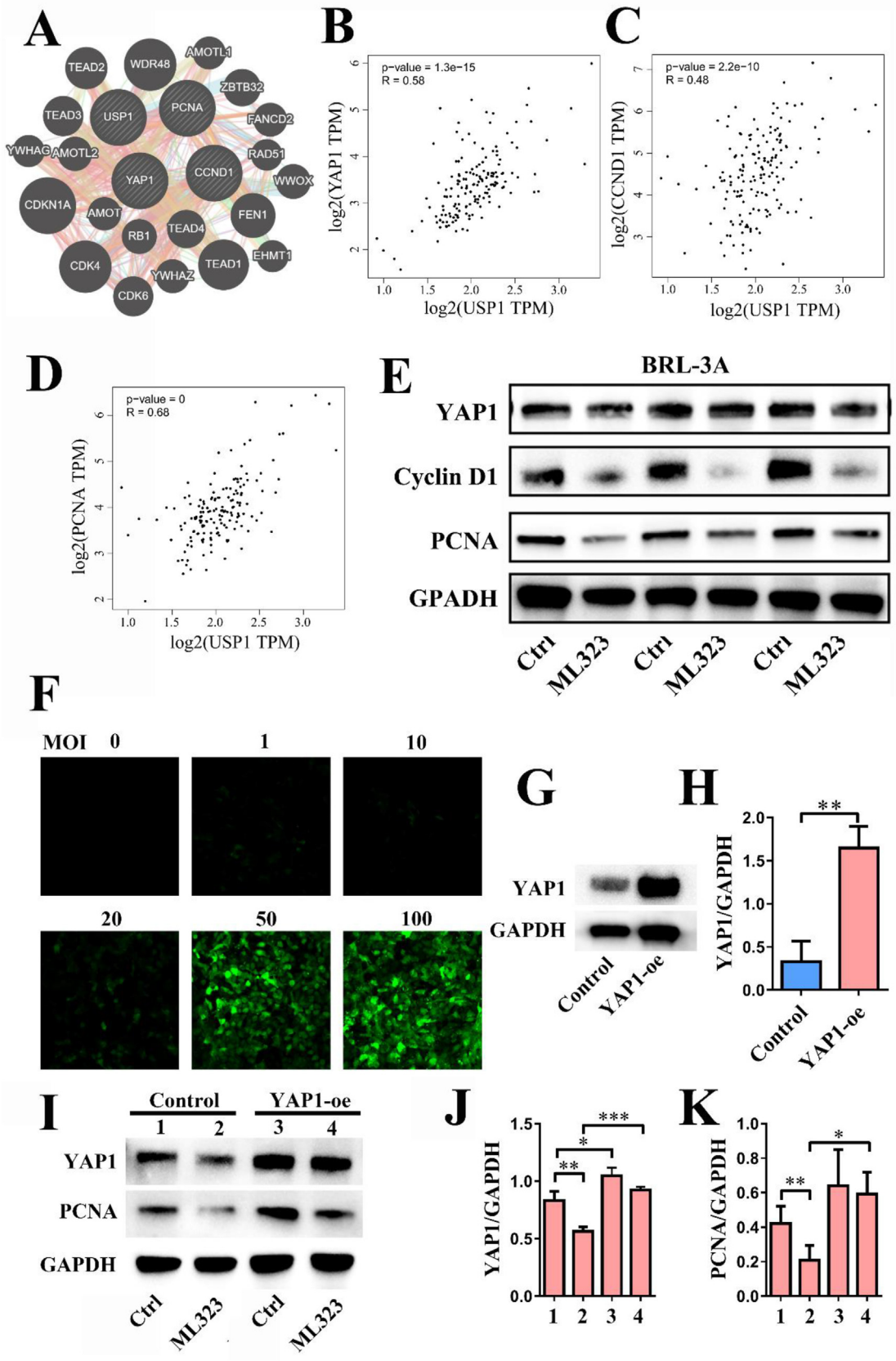

Fig. 4. Overexpression of YAP1 rescues the impairment of hepatocyte proliferation induced by ML-323. (A). GeneMina results showed the interactions among USP1 and YAP1, Cyclin D1, PCNA. (B–D). Correlation analysis between USP1 and YAP1, Cyclin D1, PCNA. (E). Protein expression of YAP1, Cyclin D1 and PCNA in Ctrl and ML-323 treated BRL3A cells. (F). Lenti-virus infection in BRL3A cells with different MOI. Enlargement: 40X. (G–H). Expression of YAP1 in Control and YAP1 overexpressed BRL3A cells. **P < 0.01. (I–K). Protein expression of YAP1 and PCNA in different groups. *P < 0.05, **P < 0.01, ***P < 0.0001.

to probe genes that were positively correlated with YAP1 in the LIHC dataset (Fig. 3C). The heatmap of the top 50 highly correlated genes was shown in Fig. 3D, such as *PTPRG*, *RNF38*, and *ROCK2* et al. The venn results in Fig. 3E showed the intersection between DEG1 and YAP1-related genes, 119 genes were selected for further analysis. Furthermore, a PPI network of these 119 genes was generated, and hub genes were identified using the CytoHubba plugin (Fig. 3F). Clustering analysis results revealed a clear distinction between the pre-PHx-Hep group and the PHx-24 h-Hep group with respect to these hub genes. Among these, USP1 ranked first (Fig. 3G). Moreover, the expression levels of these hub genes in different groups were shown in Fig. S2. KEGG enrichment analysis results showed that these hub genes were mainly enriched in the following pathways: homologous recombination, Fanconi anemia pathway, nucleocytoplasmic transport et al. (Fig. 3H). Among these, we mainly focused on the Fanconi anemia pathway, which included USP1. Generally, the Fanconi anemia pathway plays an important role in DNA crosslink repair and the maintenance of genome stability [23,24]. As shown in Fig. S3, several hub genes were involved in the Fanconi pathway, besides USP1. In addition, western blotting was performed to validate the expression of USP1 in two groups. We confirmed that USP1 was up-regulated in the PHx-24 h-Hep cells (Fig. 3I). To further confirm the association between USP1 and YAP1, we searched the GeneMINIA database to generate another PPI network. We found that *USP1*, *YAP1*, *CCND*1, and *PCNA* were tightly correlated in this network (Fig. 4A). Moreover, these correlations were also confirmed by data from the GEPIA database. Based on the Pearson correlation analysis, *USP1* showed significant positive correlations with *YAP1, CCND1,* and *PCNA* ($r > 0.4$, $P < 0.05$). We also found that the protein expression levels of YAP1, Cyclin D1, and PCNA were down-regulated in BRL3A cells after treatments with ML-323. Nevertheless, we wondered whether these down-regulations could be rescued by YAP1 overexpression. After infection with recombinant lentivirus (PGMLV-CMV-R_Yap1-EF1-ZsGreen1-T2A-Puro), YAP1 was significantly elevated in YAP1-oe BRL3A cells ($P < 0.01$) (Fig. 4F–H). Moreover, the down-regulation of YAP1 and PCNA in ML-323 treated BRL3A cells was rescued after YAP1 overexpression (Fig. 4I–K).

4.4. Validation of the effects of USP1 on liver regeneration in vivo

We found that ML-323 could significantly inhibit liver regeneration after PHx *in vivo*. After treatment with ML-323, there were no significant histological changes compared with the PHx group (Fig. 5A). However, we observed significantly decreased liver weight/body weight ratios in the PHx-ML-323 group, compared with the PHx-ctrl group ($1.59 \pm 0.05\%$ vs. $1.85 \pm 0.15\%$, $P < 0.05$) (Fig. 5B). In addition, ML-323 treatment reduced the numbers of YAP1+ and Ki67+ hepatocytes after PHx (Fig. 5A).

Our findings in this study suggest that USP1 is critically associated with YAP1 in hepatocyte proliferation during liver regeneration. Pharmacological inhibition of USP1 by ML-323 substantially impairs hepatocyte proliferation during liver regeneration (Fig. 6).

5. Discussion

In the present study, we proceeded with a series of bioinformatics analyses and identified the association between USP1 and YAP1 during the process of liver regeneration. Moreover, this finding was supported by *in vitro* and *in vivo* experiments. Hepatocyte proliferation after PHx was YAP1-dependent, and siRNA transfection or pharmacological inhibition of YAP1 significantly inhibited hepatocyte proliferation. In contrast, overexpression of YAP1 could induce hepatocyte proliferation. However, pharmacological inhibition of USP1 by ML-323 impaired liver regeneration and blocked YAP1-dependent hepatocyte proliferation. These

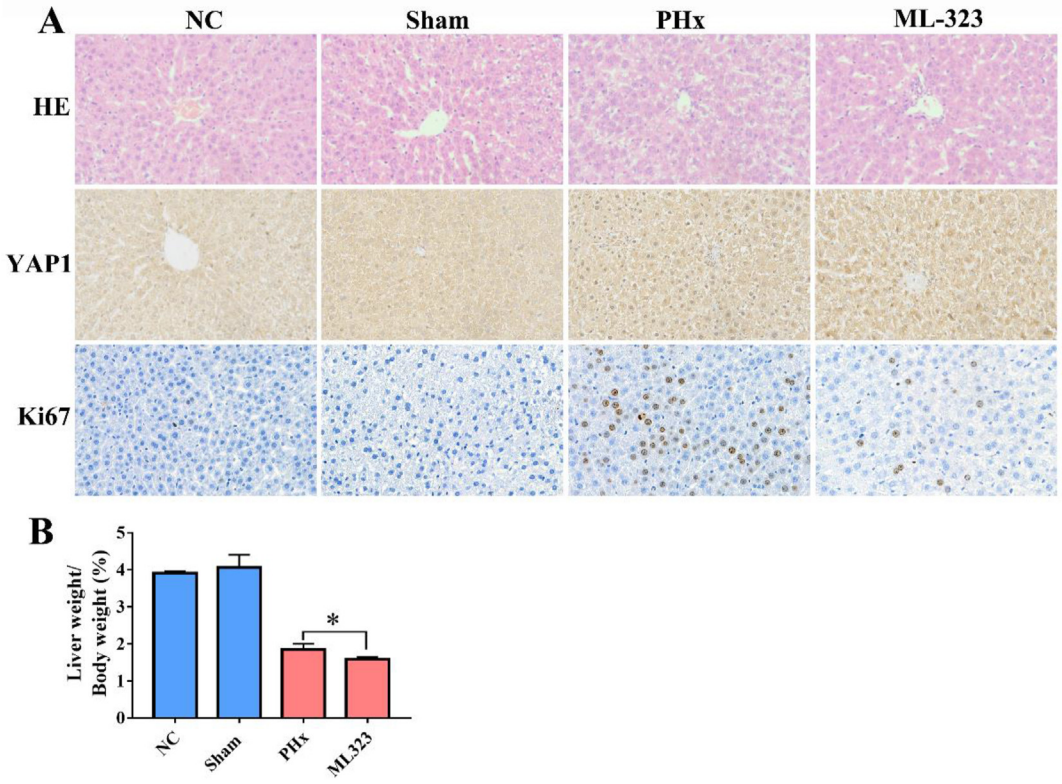

Fig. 5. ML-323 treatment inhibited liver regeneration after PHx *in vivo*. (A). Histological changes, Ki67 staining, and PCNA staining in the NC, Sham, PHx and ML-323 groups. 40 ×. (B). Liver weight/body weight ratios in the NC, Sham, PHx, and ML-323 groups. *$P < 0.005$.

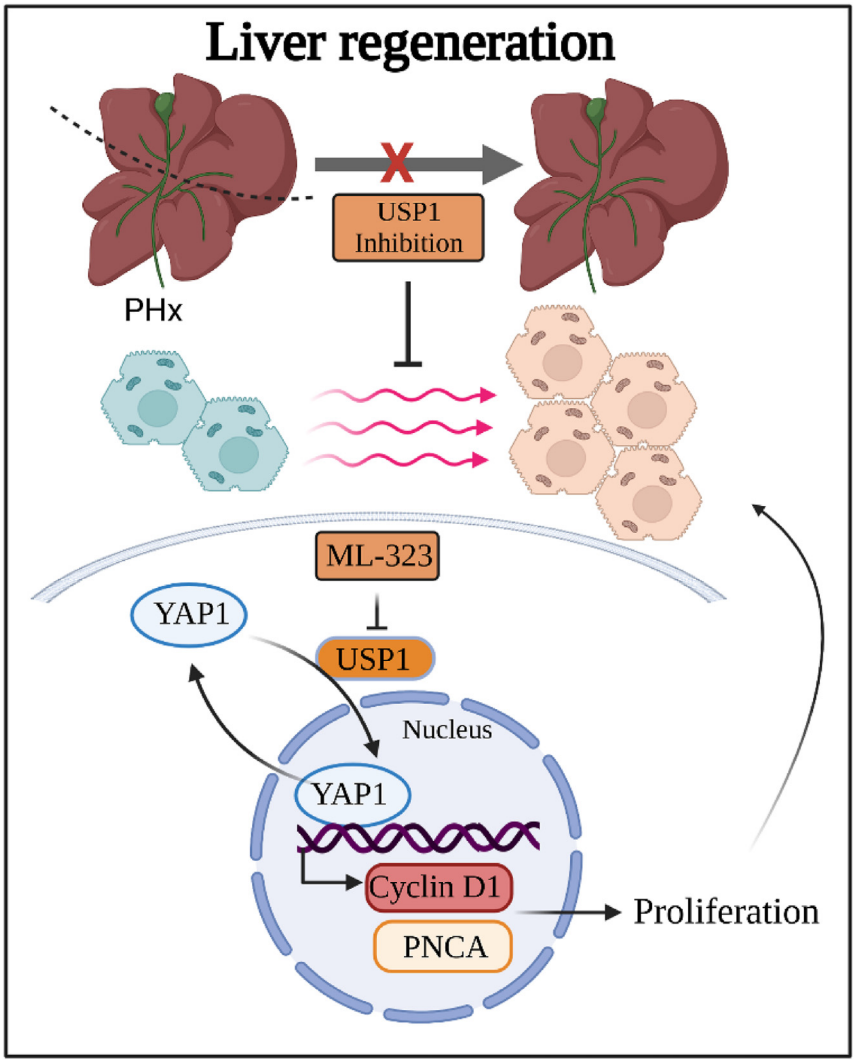

Fig. 6. Potential relationships between USP1 and YAP1 induced hepatocyte proliferation during liver regeneration. PHx: partial hepatectomy, USP1: ubiquitin specific peptidase 1, YAP1: yes-associated protein 1, PCNA: proliferating cell nuclear antigen.

findings in the present study provide us with a novel perspective on the critical regulatory role of USP1 in YAP1-dependent hepatocyte proliferation in rats.

Notably, modulation of YAP1 activation-inactivation is essential to animal development and organ regeneration. The regulatory mechanisms of the Hippo-YAP1 pathway have been specifically reviewed [4]. Among these, post-translational modification, especially ubiquitination-deubiquitination, of YAP1 is of considerable significance [25]. The balance of ubiquitination-deubiquitination is maintained by the regulation of E3 ubiquitin ligases and deubiquitinases [26]. As reported, YAP1 is directly modulated by ubiquitination-deubiquitination [27]. Growing evidence demonstrates that ubiquitin specific peptidases play vital roles in the deubiquitination and stabilization of YAP1, such as USP9X and USP10 [28–30]. In 2020, Mussell et al. identified USP1 as a novel TAZ regulator. They found that USP1 could stabilize the TAZ protein via ubiquitin modifications [31]. Recently, Yuan et al. reported that pharmacological inhibition of USP1 by ML-323 could destabilize TAZ, thus suppressing the progression of osteosarcoma [32]. Thus, the regulation of USP1 on the Hippo pathway is of great interest. Most recently, Ge et al. reported that USP1/UAF1 could stabilize METTL3, which modulates the RNA N6-methyladenosine (m6A) modification of YAP1 [33]. Consistent with these findings, we found that USP1 showed strongly positive correlations with YAP1, Cyclin D1, and PCNA. In addition, ML-323 treatment significantly reduced YAP1 protein levels. Moreover, overexpression of YAP1 could significantly reverse this reduction. These results meant that USP1 was associated with the regulation and stabilization of YAP1. Up to now, our understanding of USP1 in liver diseases is still superficial and limited. Previously, we comprehensively analyzed the vital role of USP1 in HCC and identified it as a promising therapeutic target with good prognostic value [34]. After that, researchers focused more attention on the novel functions of USP1 in HCC and other liver diseases [35–39]. Recently, Du et al. revealed that USP1 was also engaged in liver fibrosis. USP1 could significantly promote liver fibrosis via positive regulation of Snail-1 and CXCL1 [39]. These studies demonstrated that USP1 was a promising therapeutic target in various liver diseases. However, few studies have focused on USP1 in liver regeneration. Our present study took the lead in demonstrating the role of USP1 in liver regeneration. We concluded that pharmacological inhibition of USP1 impaired liver regeneration after PHx. ML-323 treatment significantly reduced the liver

weight/body weight ratios. Moreover, the impairment of liver regeneration in the ML-323 treatment group was also evidenced by the reduction of YAP1+ and Ki67+ hepatocytes. Taken together, all of these findings supported the idea that USP1 was a novel and promising therapeutic target, especially in liver regeneration. However, more studies are urgently needed to further probe the underlying mechanisms.

There are several limitations to the present study. Firstly, although USP1 is involved in liver regeneration, the functional effect of USP1 on liver regeneration may not be only via YAP1. Secondly, USP1 has been demonstrated to be involved in diverse cellular functions via deubiquitinating and stabilizing its substrates. However, whether USP1 has an impact on the ubiquitination of YAP1 is not discussed in this study. Nevertheless, our findings in the present study lay the foundation for understanding the role of USP1 in liver regeneration.

6. Conclusion

USP1 was identified as a novel therapeutic biomarker that was associated with YAP1, and pharmacological inhibition of it impaired liver regeneration.

Funding

We thank the support from the Institutional Foundation of the First Affiliated Hospital of Xi'an Jiaotong University (2021QN-05), and the Natural Science Basic Research Plan in Shaanxi Province of China (2022JQ-833).

Conflicts of interest

The authors have no conflict of interests related to this publication.

Data availability

Data will be made available on request.

Authorship contribution statement

Yalei Zhao, Fen Zhang, and Xiaoli Zhang: Conceptualization, Methodology, Investigation. Zuhong Li and Qian Li: Methodology, Formal analysis, Investigation. Tianzhi Ni and Ruojing Wang: Investigation. Liangru Liu: Resources. Yingli He and Yingren Zhao: Conceptualization, Supervision, Project administration.

Declaration of competing interest

The authors declare that they have no known competing financial interests or personal relationships that could have appeared to influence the work reported in this paper.

Appendix A. Supplementary data

Supplementary data to this article can be found online at https://doi.org/10.1016/j.reth.2023.07.004.

References

[1] Shang L, Zhao Y, Cui W. Regenerative medicine entering a new era. Small 2022;18:e2204625.
[2] Tam PKH, Wong KKY, Atala A, Giobbe GG, Booth C, Gruber PJ, et al. Regenerative medicine: postnatal approaches, the Lancet. Child & adolescent health 2022;6:654–66.
[3] de Coppi P, Loukogeorgakis S, Götherström C, David AL, Almeida-Porada G, Chan JKY, et al. Regenerative medicine: prenatal approaches, the Lancet. Child & adolescent health 2022;6:643–53.
[4] Moya IM, Halder G. Hippo-YAP/TAZ signalling in organ regeneration and regenerative medicine. Nat Rev Mol Cell Biol 2019;20:211–26.
[5] Zhao Y, Chen E, Huang K, Xie Z, Zhang S, Wu D, et al. Dynamic alterations of plasma metabolites in the progression of liver regeneration after partial hepatectomy. J Proteome Res 2020;19:174–85.
[6] Michalopoulos GK. Hepatostat: liver regeneration and normal liver tissue maintenance. Hepatology (Baltimore, Md 2017;65:1384–92.
[7] Nishina H. Physiological and pathological roles of the Hippo-YAP/TAZ signaling pathway in liver formation, homeostasis, and tumorigenesis. Cancer Sci 2022;113:1900–8.
[8] Zhao Y, Yang Y, Li Q, Li J. Understanding the unique microenvironment in the aging liver. Front Med 2022;9:842024.
[9] Tang C, Chen H, Jiang L, Liu L. Liver regeneration: changes in oxidative stress, immune system, cytokines, and epigenetic modifications associated with aging. Oxid Med Cell Longev 2022;2022:9018811.
[10] Michalopoulos GK, Bhushan B. Liver regeneration: biological and pathological mechanisms and implications, Nature reviews. Gastroenterol Hepatol 2021;18:40–55.
[11] Zou G, Park JI. WNT signaling in liver regeneration, disease, and cancer, clinical and molecular hepatology. 2022.
[12] Shu W, Yang M, Yang J, Lin S, Wei X, Xu X. Cellular crosstalk during liver regeneration: unity in diversity. Cell Commun Signal : CCS 2022;20:117.
[13] He Q, Cui L, Yuan X, Wang M, Hui L. Cell identity conversion in liver regeneration after injury. Curr Opin Genet Dev 2022;75:101921.
[14] Russell JO, Camargo FD. Hippo signalling in the liver: role in development, regeneration and disease, Nature reviews. Gastroenterol Hepatol 2022;19:297–312.
[15] Higgins G. Experimental pathology of the liver. I. Restoration of the liver of the white rat following partial surgical removal. Arch Pathol 1931;12.
[16] Jiang Z, Sun Z, Ouyang X, Zhao Y, Zhou M, Wang B, et al. Temporal integrative omics reveals an increase in nondegradative ubiquitylation during primary hepatocyte dedifferentiation. Engineering 2020;6:1302–14.
[17] Bolger AM, Lohse M, Usadel B. Trimmomatic: a flexible trimmer for Illumina sequence data. Bioinformatics 2014;30:2114–20.
[18] Sherman BT, Hao M, Qiu J, Jiao X, Baseler MW, Lane HC, et al. DAVID: a web server for functional enrichment analysis and functional annotation of gene lists (2021 update). Nucleic Acids Res 2022;50:W216–21.
[19] Vasaikar SV, Straub P, Wang J, Zhang B. LinkedOmics: analyzing multi-omics data within and across 32 cancer types. Nucleic Acids Res 2018;46:D956–63.
[20] Tang Z, Li C, Kang B, Gao G, Li C, Zhang Z. GEPIA: a web server for cancer and normal gene expression profiling and interactive analyses. Nucleic Acids Res 2017;45:W98–102.
[21] Oh SH, Swiderska-Syn M, Jewell ML, Premont RT, Diehl AM. Liver regeneration requires Yap1-TGFβ-dependent epithelial-mesenchymal transition in hepatocytes. J Hepatol 2018;69:359–67.
[22] Loforese G, Malinka T, Keogh A, Baier F, Simillion C, Montani M, et al. Impaired liver regeneration in aged mice can be rescued by silencing Hippo core kinases MST1 and MST2. EMBO Mol Med 2017;9:46–60.
[23] Ozmen Yaylaci A, Canbek M. The role of ubiquitin signaling pathway on liver regeneration in rats. Mol Cell Biochem 2023;478:131–47.
[24] Jones MJ, Huang TT. The Fanconi anemia pathway in replication stress and DNA crosslink repair. Cell Mol Life Sci : CMLS 2012;69:3963–74.
[25] Liu Y, Deng J. Ubiquitination-deubiquitination in the Hippo signaling pathway (review) Oncol Rep 2019;41:1455–75.
[26] Suresh B, Lee J, Kim KS, Ramakrishna S. The importance of ubiquitination and deubiquitination in cellular reprogramming. Stem Cell Int 2016;2016:6705927.
[27] Liu C, Cheng X, Chen J, Wang Y, Wu X, Tian R, et al. Suppression of YAP/TAZ-Notch1-NICD axis by bromodomain and extraterminal protein inhibition impairs liver regeneration. Theranostics 2019;9:3840–52.
[28] Zhu H, Yan F, Yuan T, Qian M, Zhou T, Dai X, et al. USP10 promotes proliferation of hepatocellular carcinoma by deubiquitinating and stabilizing YAP/TAZ. Cancer Res 2020;80:2204–16.
[29] Li L, Liu T, Li Y, Wu C, Luo K, Yin Y, et al. The deubiquitinase USP9X promotes tumor cell survival and confers chemoresistance through YAP1 stabilization. Oncogene 2018;37:2422–31.
[30] Mussell A, Frangou C, Zhang J. Regulation of the Hippo signaling pathway by deubiquitinating enzymes in cancer. Genes & diseases 2019;6:335–41.
[31] Mussell A, Shen H, Chen Y, Mastri M, Eng KH, Bshara W, et al. USP1 regulates TAZ protein stability through ubiquitin modifications in breast cancer. Cancers 2020:12.
[32] Yuan P, Feng Z, Huang H, Wang G, Chen Z, Xu G, et al. USP1 inhibition suppresses the progression of osteosarcoma via destabilizing TAZ. Int J Biol Sci 2022;18:3122–36.
[33] Ge X, Ye W, Zhu Y, Cui M, Zhou J, Xiao C, et al. USP1/UAF1-stabilized METTL3 promotes reactive astrogliosis and improves functional recovery after spinal

cord injury through m(6)A modification of YAP1 mRNA. J Neurosci : the official journal of the Society for Neuroscience 2023;43:1456–74.
[34] Zhao Y, Xue C, Xie Z, Ouyang X, Li L. Comprehensive analysis of ubiquitin-specific protease 1 reveals its importance in hepatocellular carcinoma. Cell Prolif 2020;53:e12908.
[35] Li Y, Xu Y, Gao C, Sun Y, Zhou K, Wang P, et al. USP1 maintains the survival of liver circulating tumor cells by deubiquitinating and stabilizing TBLR1. Front Oncol 2020;10:554809.
[36] Liao Y, Shao Z, Liu Y, Xia X, Deng Y, Yu C, et al. USP1-dependent RPS16 protein stability drives growth and metastasis of human hepatocellular carcinoma cells. J Exp Clin Cancer Res : CR 2021;40:201.
[37] Chen Z, Ma Y, Guo Z, Song D, Chen Z, Sun M. Ubiquitin-specific protease 1 acts as an oncogene and promotes lenvatinib efficacy in hepatocellular carcinoma by stabilizing c-kit. Ann Hepatol 2022;27:100669.
[38] Lu Z, Zhang Z, Yang M, Xiao M. Ubiquitin-specific protease 1 inhibition sensitizes hepatocellular carcinoma cells to doxorubicin by ubiquitinated proliferating cell nuclear antigen-mediated attenuation of stemness. Anti Cancer Drugs 2022;33:622–31.
[39] Du Z, Wu T, Liu L, Luo B, Wei C. Ubiquitin specific peptidase 1 promotes hepatic fibrosis through positive regulation of CXCL1 by deubiquitinating SNAIL, Digestive and liver disease. official journal of the Italian Society of Gastroenterology and the Italian Association for the Study of the Liver 2022;54:91–102.